


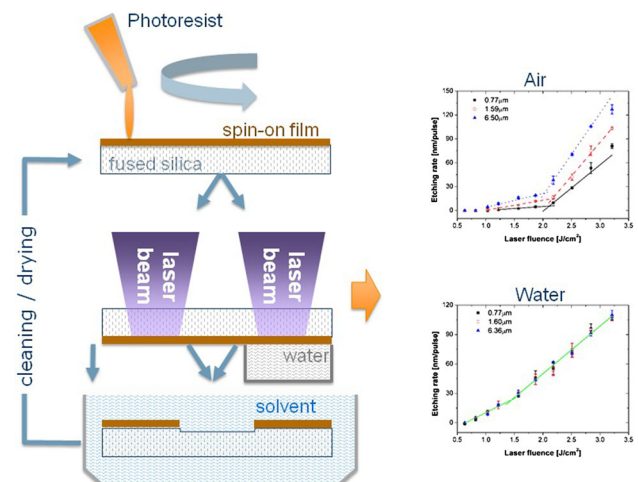
Influence of the confinement on laser-induced dry etching at the rear side of fused silica

Yunxiang Pan^{1,2} · Martin Ehrhardt² · Pierre Lorenz² · Bing Han³ · Bela Hopp⁴ · Csaba Vass⁴ · Xiaowu Ni¹ · Klaus Zimmer² 

Received: 30 September 2015 / Accepted: 23 February 2016 / Published online: 14 March 2016
© Springer-Verlag Berlin Heidelberg 2016

Abstract Laser-induced etching at the rear side of transparent material enables high-quality machining results. However, the mechanism is still not completely recognized which would allow further optimization. Therefore, multi-pulsed laser-induced backside dry etching with different thick photoresist films was studied experimentally for air (MP-LIBDE) and water confinements (cMP-LIBDE). The water confinement causes differences in photoresist ablation morphology and etching rate in dependence on laser fluence, film thickness and pulse number. Owing to the water confinement, the extent of photoresist film spallation and the etching rate slope difference in low and high fluence ranges are reduced. In particular, the etching rate of cMP-LIBDE keeps constant with different film thicknesses in contrast to MP-LIBDE. Two effects that are related to the water confinement, mechanical confinement and heat transfer alterations, are analysed and discussed in relation to the differences between MP-LIBDE and cMP-LIBDE.

Graphical Abstract



1 Introduction

Inorganic transparent materials can be used to manufacture micro-fluidic and micro-optical elements due to their high chemical stability and high transmittance over a large range of wavelength. Various methods of direct machining these materials using UV-lasers with nanosecond duration are excluded in consequence of the high surface roughness and the possibility of crack formation after laser machining. Further, to induce laser ablation, very high laser fluences should be applied. Hence, alternative methods of introducing sufficient absorbance at the rear side of the transparent materials [1–4] by applying additional materials (absorber) or laser-induced plasma from metal targets placed just behind the transparent materials (LIPAA) [5]

✉ Klaus Zimmer
klaus.zimmer@iom-leipzig.de

¹ School of Science, Nanjing University of Science & Technology, Xiaolingwei 200, Nanjing 210094, China

² Leibniz-Institute of Surface Modification, Permoserstr. 15, 04318 Leipzig, Germany

³ Advanced Launching Co-innovation Centre, Nanjing University of Science & Technology, Xiaolingwei 200, Nanjing 210094, China

⁴ Department of Optics and Quantum Electronics, University of Szeged, Dómtér 9, Szeged 6720, Hungary

are intensively studied to etch high-resolution structures. By these means, a good surface quality and a crack-free etched surface can be achieved with relative low laser fluence.

Laser backside etching using different absorber materials can be classified into laser etching at a surface-absorbed layer (LESAL) [1, 2], laser-induced backside wet etching (LIBWE) [3] and laser-induced backside dry etching (LIBDE) [4] according to the state of the attached absorber. LIBWE, where an organic solvent with high absorption at the laser wavelength is attached at the back side of the sample, is characterized by incubation effects, a comparable low etching rate and a low surface roughness. In LIBDE, metal films are often coated at the rear side of the sample, and non-incubation effects and high etching rate are the most remarkable features, but the etching depth is limited due to the removal of film at etching. Processes of surface melting and evaporation, plasma heating, shock-wave impact and modified layer deposition at the interface are all involved in LIBWE and LIBDE. But for LIBWE, the process of bubble oscillation should be considered for the high pressure and temperature fields accompanied with bubble collapse [6].

The very complex mechanism of laser-induced backside etching processes requires the simplification of the process or comparative experiments to focus the study on one detail. The main differences between LIBWE and LIBDE are the absorber materials and confinement conditions. Hopp [7] compared the etching behaviour of LIBWE and LIBDE by using molten tin droplets and thin tin films, respectively. The experimental results show no significant difference in that case, which indicates that the mechanism of metallic LIBWE and LIBDE is similar. The influence of specific confinement conditions on LIBDE has been investigated for thin carbon films [8] and thin chromium films [9]. When carbon layer is used as absorber, the water confinement is demonstrated to change the dependence of etching rate on laser fluence from rate saturation to linear growing. When chromium film is deposited at the rear surface of sample, the existence of water confinement leads to a lower etching rate, higher etching threshold and lower etching depth. However, systematic studies of the influence on the confinement on the etching result have not been executed yet.

Laser rear side etching experiments with adjustable confinement conditions are hardly to perform with the standard LIBWE etching conditions. One opportunity is to stack thicker organic absorber films at the rear side of the transparent, functional material. Hence, the optical absorption and the confining conditions can be provided by different material stacks for a first approach. In these experiments, different solid absorber films are combined with an air or a water confinement to study the

influence of the confinement for different thick photoresist films in more detail. In order to provide the same laser irradiation configuration for each laser pulse, the laser-ablated absorber film was replaced by a fresh photoresist layer after each laser pulse, which also solves the problem of etching depth saturation at LIBDE. This multi-pulse LIBDE approach can provide also a bridge for comparison of experimental etching results of LIBWE (liquid absorber; multi-pulse) with the MP-LIBDE results now achieved.

In this work, comparative experiments are proposed and performed to study the influence of the confinement on laser backside etching processes. Further, the etching behaviour of fused silica with a spin-on photoresist film of different thicknesses under air and water confinements are studied in comparison. The results can progress the understanding of the mechanism at all and the involved processes. This is a contribution to improve the model of laser etching to allow an optimization of the process for ultra-precision machining of transparent materials.

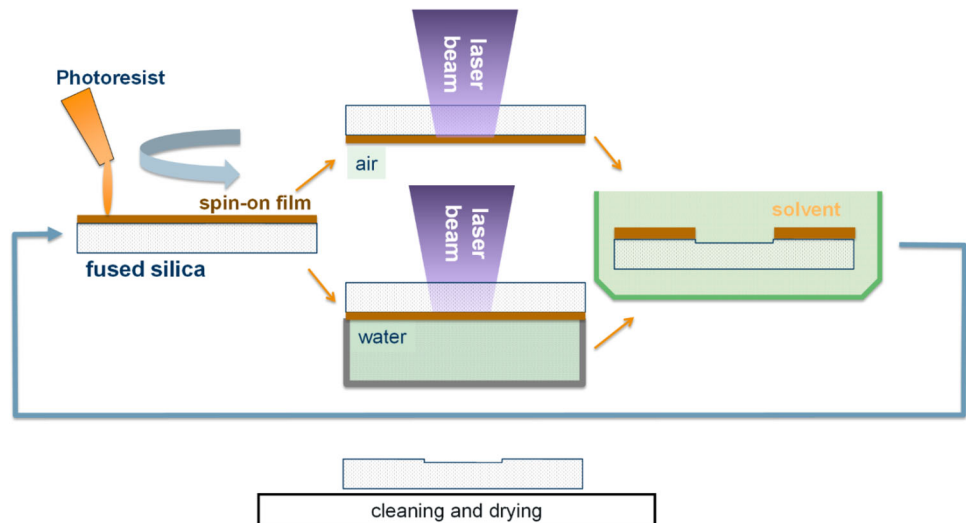
2 Experimental set-up and methodology

The methodology as well as the experimental set-up for the film preparation and the laser irradiation is shown in Fig. 1. For differentiating the influence of laser beam absorption and laser material interaction confinement, one set of the parameters has to be kept constant while the other is changed. For changing the confinement, two different approaches are followed: one is the changing of the film thickness and the other is the adding of a liquid confinement medium to the rear side of the absorbing film. In the current investigations, we applied only a bulk water confinement instead of air.

The methodology for providing a new absorbing thin film for subsequent laser pulses is already described in Ref. [10]. Briefly, first a homogeneous photoresist film was deposited by a standard spin-on process that was allowed subsequently to dry for 1 min at 100 °C. Thereafter, the samples were flipped and laser-irradiated through the fused silica substrate with one laser pulse. Before a new resist film was deposited, the fused silica samples were cleaned from the already laser-irradiated film with solvents. The confinement of the interaction process is changed by applying a non-absorbing liquid in addition to the absorbing film to the sample's rear side.

A KrF excimer laser with a wavelength of 248 nm and a pulse width of 24 ns was focused at the interface of the fused silica wafer and the thin resist film, as shown in Fig. 1. After the final etching, the sample was cleaned step by step in sequence with imaging the surface of the etchings. In particular, white light interference microscopy (WLIM) and secondary electron microscopy (SEM) were applied for

Fig. 1 Experimental set-up and methodology for the studies of the multi-pulse laser etching experiments with organic absorber films at different confinement conditions



selected etchings. Finally, the samples were cleaned with microwave air plasma for 1 min. Only a low energy of the ions from the plasma can be expected due to the high pressure of the plasma. However, the excited oxygen is able to burn off all organic materials; hence, a high selectivity for the cleaning abilities to organic materials can be expected. With these means, the characteristics of the laser etching process as well as the surface morphology with and without confinement can be directly compared.

A laser fluence range of 0.63–3.21 J/cm² which covers the near-threshold fluence, stable etching fluence and high fluence ranges of LIBWE [11] was chosen for irradiation the rear surface of fused silica. Photoresist films with thicknesses of 0.20, 0.77, 1.59, 2.91, 6.50 and 11.70 μm for air confinement and 0.77, 1.60, 6.36 μm for water confinement were prepared. Within these experiments, the laser etching was stopped after eight pulses were accumulated on the same site.

To allow all measurements after etching an array of N columns (number of laser fluences), M rows (number of pulses) were prepared, and after applying a new photoresist film the finished rows (already done pulse numbers) are skipped. Hence, for each parameter set, the surface morphology and the etching rate can be measured in detail. The etching rate was calculated from dividing the final etching depth by the applied pulse number for air and water confinements.

3 Results

Figure 2 shows the optical images of the rear side of the sample taken immediately after the laser etching procedure finished. Both the ablated photoresist and the etched square into the fused silica can be seen. Results of different

confinements, namely air confinement and water confinement, are shown in Fig. 2a, b, respectively. In general, the size and the shape of the etchings and the modifications of the fused silica correlate almost with the laser spot for all experiments. At low laser fluences and thin film thickness, the shape of the ablated photoresist is also close to the square laser spot. The size of the ablated photoresist increases and the shape becomes heavily rounded in the case of air with increasing laser fluence and comparatively less pronounced with rising film thickness. However, due to the confinement of water, the increase in the ablation-affected zone driven by the growth of laser fluence and film thickness is reduced; also its shape stays more square with jagged edges when extending outward.

The SEM images of Fig. 3 show etchings of a fused silica surface in comparison with and without water confinement. As the other etching parameters are almost the same, the morphology can be directly compared. The waviness on the bottom of the etched site is observed for both air and water confinements. Taking into account the remaining beam inhomogeneities, the waviness of the etched surface can be attributed to the limited beam quality. A significant difference in the surface quality of the etched surface cannot be observed.

The etching depth as an important characteristic was measured in dependence on the laser fluence, film thickness and the pulse number for different confinements to study the influence of confinement conditions on the etching rate. First, the effects of laser fluence on etching rate are studied for MP-LIBDE and cMP-LIBDE. Figure 4 shows the results for eight laser pulses, three different film thicknesses as well as the two confinement conditions (air, water). In general, a clear difference between water and air confinement in terms of the etching behaviour, etching rate, the etching slopes and the surface morphologies is seen.

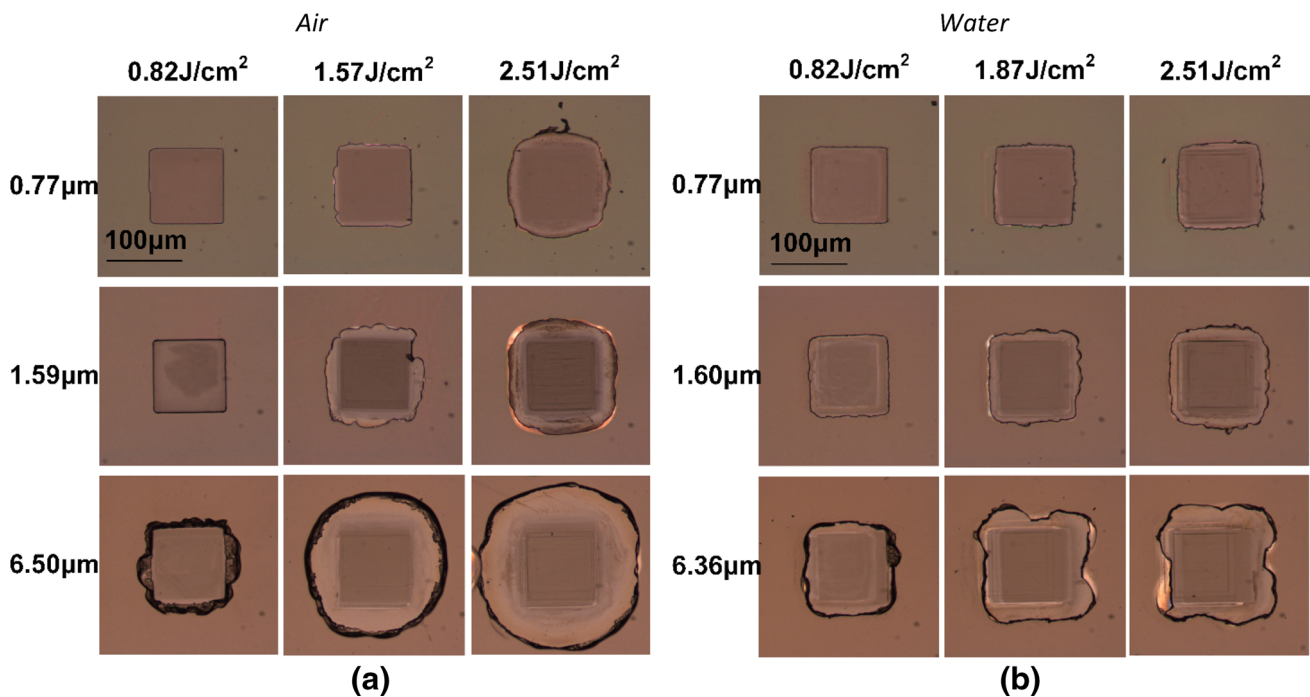


Fig. 2 Comparison of optical images of the surface morphology of laser-etched fused silica samples at different confinement (air, water) still having the photoresist film from the last MP-LIBDE on top. Eight laser pulses and similar film thicknesses (approx. 0.77, 1.6 and 6.5 μm) and laser fluences were used for comparison of air and water

confinements. Without **a** water confinement larger and rather *circular-shaped* photoresist delamination is seen whereas with water confinement **b** the photoresist delamination is smaller and maintains *square*

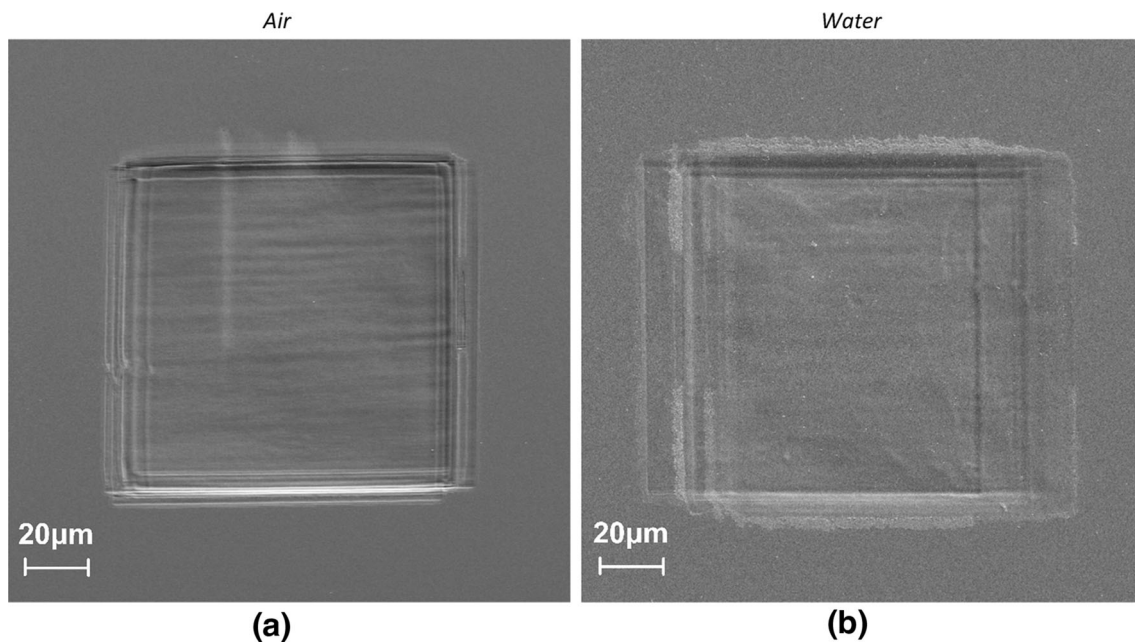


Fig. 3 SEM images of the surface morphology of fused silica samples with a 1.60- μm -thick photoresist film laser-etched **a** without and **b** with water confinement after eight laser pulses were accumulated. The applied laser fluence is 3.21 J/cm^2

Similar to MP-LIBDE, the etching rate slope at cMP-LIBDE can be separated into two fluence ranges with a lower slope in low fluence range compared to high

fluences. However, the difference in the slopes is much higher without the water confinement. Further, three features are different when comparing MP-LIBDE and cMP-

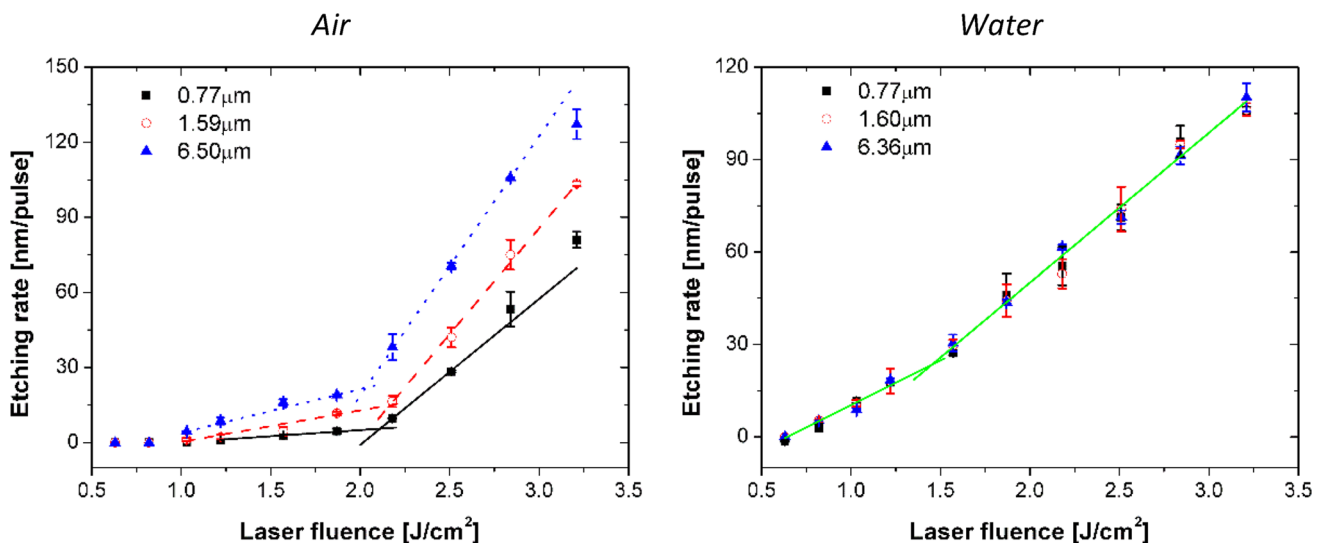


Fig. 4 Etching rate of fused silica samples in dependence on the laser fluence for eight laser pulses ($N = 8$) without and with water confinement for 0.77, 1.59 and 6.50- μm -thick photoresist films

LIBDE. First, an influence of film thickness on etching rate cannot be observed at cMP-LIBDE as the three coinciding curves in Fig. 4b show. Second, the threshold fluence of water confinement is estimated to be 640 J/cm^2 , which is obviously lower than that of air confinement. The corresponding thresholds at MP-LIBDE for 0.77, 1.59 and 6.50 μm films are 990, 790 and 740 J/cm^2 , respectively. All of the threshold fluences are obtained by extrapolating the linear fit of the etching rate measured for low fluences (see Fig. 4). This approach is commonly used to define the threshold and is believed to be very close to the exact threshold [16], although it is possible that the growth of the etching rate is not linear at etching threshold. Further, the slope of cMP-LIBDE is higher than MP-LIBDE in low fluence range, but lower in high fluence range. Hence, the magnitude of the slope change with rising fluence is not as apparent as MP-LIBDE.

The dependence of etching rate on film thickness of MP-LIBDE and cMP-LIBDE is shown in Fig. 5. The etching rate of MP-LIBDE first increases at thin thickness range and goes to a saturation at 2.9 μm as shown in Fig. 5a. Different with MP-LIBDE, Fig. 5b indicates that the etching rate of cMP-LIBDE is unchanged with the film thickness. However, the currently almost independence of the etching rate from the film thickness at cMP-LIBDE can be explained by the minimum film thickness 0.77 μm that is much larger than the optical penetration depth of 0.23 μm . Hence, experiments of cMP-LIBDE with thinner films should be conducted to get more comprehensive information. In contrast to that, MP-LIBDE shows strong film thickness dependence although the absorbed energy is also independent on the film thickness and keeps constant. It has to be noticed that at MP-LIBDE the rate increased by

one order of magnitude (without changing the absorbed energy) and the reached value at 12- μm film thickness is similar that of cMP-LIBWE.

Figures 4 and 6 show the dependence of etching rate on pulse number for MP-LIBDE and cMP-LIBDE. Similar to MP-LIBDE, the averaged etching rate of cMP-LIBDE grows with the number of pulses and goes into stable etching when a sufficient pulse number is accumulated. However, the three coincident graphs for cMP-LIBDE again confirm that etching rate of cMP-LIBDE is not influenced by the film thickness within the investigated thickness range. In contrast, thicker film leads to a higher etching rate at MP-LIBDE. However, when the film thickness is high enough ($d = 6.36 \mu\text{m}$), the averaged etching rate can reach the rate of cMP-LIBDE. Laser fluencies higher than 2.51 J/cm^2 can result in even higher rates exceeding that of cMP-LIBDE, since the growth rate of etching rate after the inflection point is much higher than cMP-LIBDE (see Fig. 4). Although incubation effects are observed in all cases, these effects are more expressed in the case of air confinement. Moreover, unlike in other cases of MP-LIBDE, 6 μm films show an almost stable etching with the first laser.

The optical images in Fig. 7 show clearly a surface modification around the laser-etched laser spots. The characterization of the laser modification is needed especially to reveal the contribution of the surface modification to the etching process. In particular, the interaction of the surface modification with the laser photons can be important for the laser etching process.

The surface modifications after completing the laser etching and dissolving the photoresist that remain at the sample surface at least in parts are seen in the optical images (see Fig. 7).

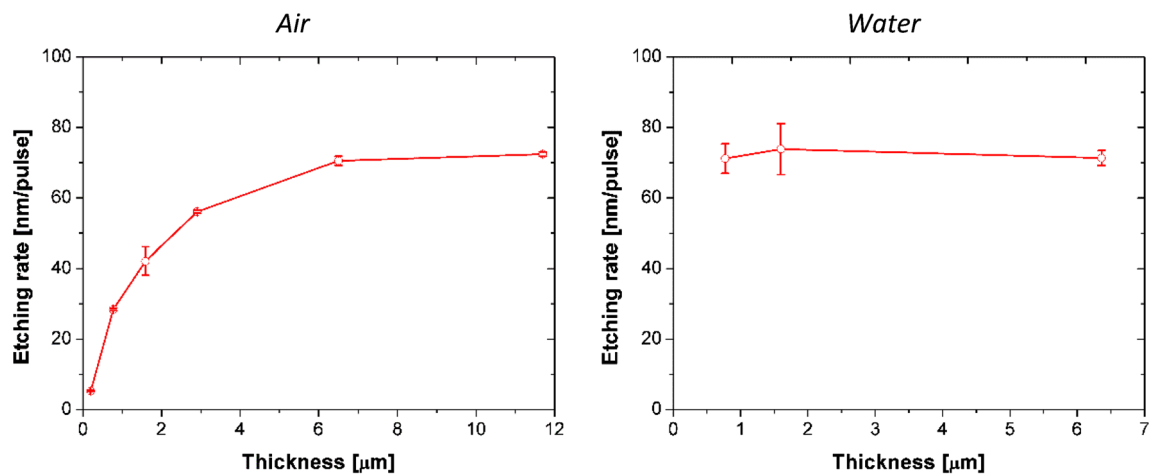


Fig. 5 Etching rate of fused silica samples in dependence on film thickness without and with water confinement with laser fluence of 2.51 J/cm^2 and eight pulse numbers

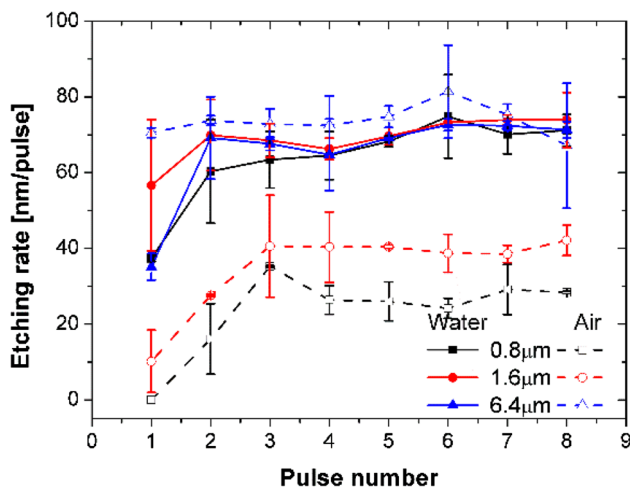


Fig. 6 Average etch rate as a function of the pulse number for three different film thicknesses of 0.8, 1.6 and $6.4 \mu\text{m}$, respectively, and the applied laser fluence is 2.51 J/cm^2

The transition of predominant surface modification within the laser spot to outside the laser spot is approximately 1.03 J/cm^2 for air confinement and approximately 0.82 J/cm^2 for water confinement with the parameters of $N = 8$, $d = 1.60 \mu\text{m}$. The transition fluence is heavily affected by pulse number for both air and water confinements but affected by film thickness only for air confinement. Higher pulse number and thicker photoresist lead to lower transition fluence.

The brighter appearance gives evidence for a higher refractive index of either a deposited film or the surface. As the modifications fit the delamination range at low and high fluences and the strength of the surrounding modifications growth with the pulse number a deposited film can be expected. In a set of experiments, an additional laser pulse with a laser fluence of 2.88 J/cm^2 was applied at the back

side of the substrate across the laser-etched area cleared from the photoresist. (see Fig. 7) The brighter areas due to the modifications can be removed by an additional pulse both inside and outside the etched laser spot, respectively. That means that the surface modifications should have a rather high absorption.

Further, the ablation depth due to the additional after the laser etching applied laser pulse that was measured by WLIM is shown in Fig. 8 in dependence on the laser fluence for air confinement. The ablation depth of this single pulse is almost constant up to $\sim 1.8 \text{ J/cm}^2$ and increases thereafter very steep. The ablation depth within the low fluence region is approx. 20 nm. The transition to much higher ablation rates suggests a different mechanism of the laser modification during laser etching with fluencies above 2 J/cm^2 .

The characteristic of two slopes separated by low and high fluences in MP-LIBDE indicates different etching mechanisms. Assuming that with the additional laser pulse almost the whole modified fused silica is ablated, the thickness of the modification due to laser etching can be approximated. This assumption is supported by the fact that the laser ablation threshold of fused silica is larger than 10 J/cm^2 at 248 nm excimer laser pulses [12]. Comparing the single-pulse ablation depth with typical laser ablation rates of fused silica that are in the range of several 100 nm, the surface modification from laser etching is rather the result of a mechanism related to laser ablation than that of laser etching. The fluctuation of the single-pulse ablation depth (see error bars in Fig. 8) above 2 J/cm^2 is much higher than at low fluences. This suggests a single-pulse ablation mechanism that is defect-related at high fluences and at low fluences related to a stable surface modification. Such defect-related mechanism is typical for laser ablation whereas laser etching is related to a defined

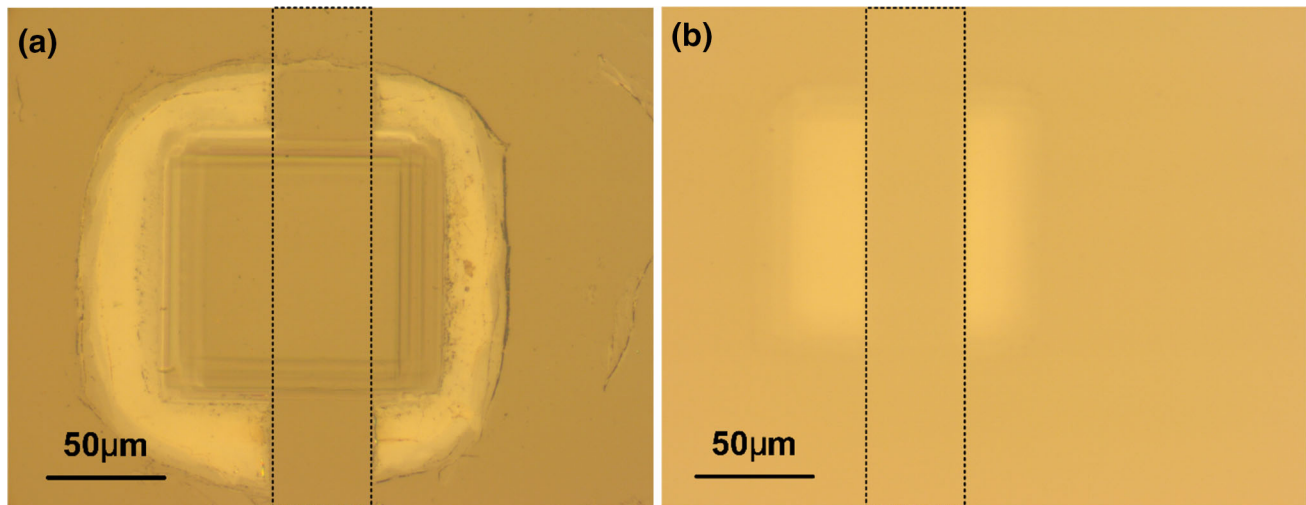


Fig. 7 Optical images of laser-etched fused silica with the additional applied laser pulse of a fluence of 2.88 J/cm^2 and a *rectangular shape* across the laser-etched area. The single laser pulse causes the removal

of the surface modification at high fluences **a** outside the square laser-etched area and at low fluences **b** inside the laser-etched area

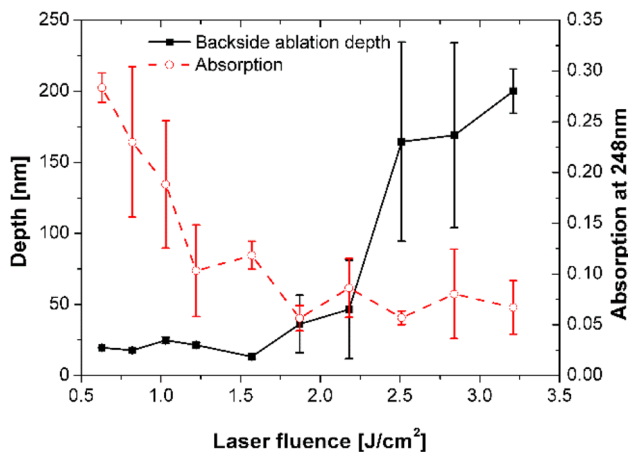


Fig. 8 Absorption of laser-etched fused silica and backside ablation depth for air confinement in dependence on the laser fluence. The film thickness and pulse number are $1.59 \mu\text{m}$ and 8, respectively

modified surface (see Ref. [13]). Hence, three fluence ranges of surface modification are also valid for MP-LIBDE.

In addition to the single-pulse ablation depth, the transmittance of the etched sites was measured and normalized to the pure fused silica reference for calculation of the absorption in dependence on the laser fluence that is also shown in Fig. 8. The absorption within the spots is highest at lowest fluence, decreases with laser fluence until approx. 1.75 J/cm^2 , and keeps nearly constant further on. The found behaviour is opposite to that of the single-pulse ablation depth (see Fig. 8).

4 Discussion

The absorption of the whole laser energy within the photoresist for all film thicknesses is ensured as the photon penetration depth is $0.23 \mu\text{m}$ for 248 nm . Hence, the observed dissimilarities for the various experimental conditions are not due to differences in the absorbed laser energy that drives the etching. Therefore, the strong influence of the photoresist film thickness and the water confinement let suggest that the effects related to the confinement are responsible for the experimental observations.

The optical images of Fig. 2 show similar cleaved photoresist film edges for air and water confinements. Similar to air confinement (see Ref. [10]), there is almost no sign of melting except the interface of the photoresist to the fused silica. Both the molten photoresist at the interface and the fracture of the photoresist edges are most likely the result of thermal expansion of the laser-heated material and/or the pressure of the expanding laser ablation products that build up a stress within film. However, the shape and the distance of the fracture from the mask edge are significantly differed between water and air, in particular for thick resist films. Supposing that for both cases a specific stress must be achieved, the round-shaped fracture can be interpreted as the bending of the photo resist in consequence of the formation of a bubble at the interface between the photoresist and the fused silica. The more square edges at water confinement are not coincident with a spherical bubble. Possible reasons for the shape at water confinement are:

1. Delay of the stress formation within the photoresist due to the water confinement that hinders the growth of the bubble.
2. Damage of the photoresist due to shockwaves from the square-shaped laser impact.
3. Cooling and delayed cracking of the photoresist.

The laser-induced modifications of the substrate surrounding the etchings due to laser plume probably depend on the amount of material and the interaction time. Comparing air and water confinements at high film thickness and high laser energy, the stronger modification outside of the laser spots at air confinement suggests longer interaction times or higher interaction intensities. Due to the similar etching rates for air and water, the initial amount of mass is similar so that the laser plasma plume density is probably responsible for the observation. Hence, immediately after the laser pulse, the bubble grows in the case of air. The less modification surrounding area in the case of water suggests a shorter laser plume interaction time meaning a slower expansion of the interface bubble that can be interpreted as mechanical effect of the confinement by the water. This longer interaction of the tightly compressed bubble probably results at least in a stronger modification of the laser spot surface. This stronger modification inside the spot can be responsible for the higher etching rates in the medium fluence range at water confinement. Further, this delay of bubble expansion allows thermal diffusion into the substrate and the photoresist film whereby the energy of the bubble drops down. In consequence of the thermal diffusion and the lower energy within the bubble, the rupture of the photoresist film is closer to the laser spot edges (see Fig. 2).

Further, the heating of the photoresist due to the longer interaction times can reduce the strength of the photoresist (glass transition temperature ~ 200 °C) so that fracture within the area of a strong thermal gradient outside of the laser-heated spot can be assumed as both thermal and mechanical stress combinations.

The configuration of cMP-LIBDE is similar to LIBWE except for the solid absorber. The two typical features of etching rate growth with two slopes as well as the incubation effects for LIBWE [14–16] are also observed in cMP-LIBDE. In comparison of cMP-LIBDE and H-LIBWE (hydrocarbon LIBWE), that provide both strong confinement, etching threshold fluencies of ~ 640 mJ/cm² (8 pulses) and 520 mJ/cm² (10 pulses) have been measured, respectively. This similar value suggests also similar processes for surface modification within the laser spot despite that the absorption coefficient of photoresist (4×10^4 cm⁻¹) is larger than the hydrocarbon solution applied in Ref. [17] (2.2×10^4 cm⁻¹).

With this suggested similar etching mechanism that is supported by similar etching behaviour and similar smooth-etched surfaces, the material removal process seems to be similar to LIBWE and mainly related to laser ablation of a strongly modified fused silica surface. This is strongly supported by the ablation experiments after laser etching (see Fig. 8). Similar to LIBWE, here at cMP-LIBDE at low fluencies (< 2 J/cm²) stable, low rate and for higher fluencies (> 2 J/cm²) a rather high rate with fluctuations are found.

Hence, three possibilities for surface modification can be discussed for cMP/MP-LIBDE:

1. Surface-adherent decomposition products of the photoresist (outside the laser-etched spot above and inside below the etching threshold) that do not enable surface modification-initiated ablation process.
2. Near-surface modifications of the fused silica due to processes of the interaction of the decomposition products of the laser-ablated hydrocarbon film with the fused silica at medium laser fluencies that enable laser etching.
3. Material-inherent, defect-related material modifications that are related to regular processes of laser ablation of not modified bulk material.

In comparison with the results reported in Ref. [9], where the etching rate of water-confined LIBDE for chromium film is lower than for LIBDE in the whole tested fluence range and the surface morphologies of the etched surface is different, not only the water confinement but also the behaviour of the absorber must be discussed. So in comparison with LIBWE and the cMP-LIBDE, the properties of chromium must be considered that has a high thermal conductivity, shows melting and does not suffer from decomposition.

Therefore, the presence of water confinement makes difference in photoresist fracture and etching rate in dependence on laser fluence, film thickness and pulse number for the current experiments, but in general additional processes must be considered.

5 Conclusion

The influence of different confinement conditions at multi-pulse LIBDE with different thick photoresist films that were studied experimentally proved that the confinement influences strongly the etching rate and the surface morphology. In particular, the laser ablation-induced photoresist spallation changed from square to round shapes for high film thickness and high laser fluence, and the etching rate is heavily influenced by film thickness at air confinement whereas with the water confinement the fractured

shape is more restricted to square and the etching behaviours of different thick films show no difference. In consequence, the confinement probably influences the mechanism of back side laser etching.

Although the influence of the increasing film thickness is clearly seen the strength of the water confinement is much higher. In particular, the linearization of the etching rate can be attributed to the confinement effect; a similar linear etching rate is typical for LIBWE that holds the same potential for strong confinement due to the applied bulk liquid at the rear side of the transparent material [8]. In relation to the differences in the rear side etching-related surface modifications seen outside the laser spot, the results strongly suggest that with higher confinement less modifications outside the laser spot occur. Also, this result is in agreement with former results of LIBWE [18, 19], where almost no modification appears, and LESAL [1], where considerable surface modifications have been found.

The comparison of the experimental result with and without water confinement enhanced the knowledge of the role of the confinement on laser processing. However, to highlight even more these questions confinement experiments with different liquid film thicknesses are in progress.

Acknowledgments The authors wish to acknowledge the help of Mrs E. Salamatın with the interference microscopic measurements and for careful reading of the manuscript and Mrs. I. Herold for supporting in preparation of the films. This work was financially supported in parts by the Deutsche Forschungsgemeinschaft, the European Union, and the European Social Fund through project Supercomputer, the national virtual lab (Grant no.: TAMOP-4.2.2.C-11/1/KONV-2012-0010) and the DAAD (no.: 56266271). Further, the Fundamental Research Funds for the Central Universities (No. 30915015104), the National Natural Science Foundation of China for Young Scholars (No. 11402120) and the Jiangsu Natural Science

Foundation for Young Scholars (No. BK20140796) provide financial support.

References

1. R. Böhme, K. Zimmer, *Appl. Surf. Sci.* **239**, 109 (2004)
2. K. Zimmer, R. Böhme, B. Rauschenbach, *Appl. Phys. A Mater. Sci. Process.* **79**, 1883 (2004)
3. J. Wang, H. Niino, A. Yabe, *Appl. Phys. A* **69**, S271 (1999)
4. B. Hopp, C. Vass, T. Smausz, *Appl. Surf. Sci.* **253**, 7922 (2007)
5. J. Zhang, K. Sugioka, K. Midorikawa, *Appl. Phys. A* **67**, 545 (1998)
6. W. Soliman, T. Nakano, N. Takada, K. Sasaki, *Jpn. J. Appl. Phys.* **49**, 116202 (2010)
7. B. Hopp, T. Smausz, C. Vass, G. Szabó, R. Böhme, D. Hirsch, K. Zimmer, *Appl. Phys. A* **94**, 899 (2009)
8. R. Böhme, K. Zimmer, B. Rauschenbach, *Appl. Phys. A* **82**, 325 (2006)
9. K. Zimmer, M. Ehrhardt, P. Lorenz, X. Wang, C. Vass, T. Csizmadia, B. Hopp, *Appl. Surf. Sci.* **302**, 42 (2014)
10. Y. Pan, M. Ehrhardt, P. Lorenz, B. Han, C. Vass, X. Ni, K. Zimmer, *Appl. Surf. Sci.* **359**, 449 (2015)
11. K. Zimmer, M. Ehrhardt, R. Böhme, Laser ablation in liquids, in *Principles and Applications in the Preparation of Nanomaterials*, ed. by G. Yang (CRC Press, Boca Raton, 2012), p. 1032
12. J. Ihlemann, B. Wolff, P. Simon, *Appl. Phys. A* **54**, 363 (1992)
13. K. Zimmer, R. Böhme, M. Ehrhardt, B. Rauschenbach, *Appl. Phys. A* **101**, 405 (2010)
14. G. Kopitkovas, T. Lippert, C. David, A. Wokaun, J. Gobrecht, *Microelectron. Eng.* **67**, 438 (2003)
15. X. Ding, Y. Kawaguchi, H. Niino, A. Yabe, *Appl. Phys. A* **75**, 641 (2002)
16. M. Ehrhardt, G. Raciukaitis, P. Gecys, K. Zimmer, *Appl. Surf. Sci.* **256**, 7222 (2010)
17. R. Böhme, A. Braun, K. Zimmer, *Appl. Surf. Sci.* **186**, 276 (2002)
18. K. Zimmer, R. Böhme, D. Ruthe, B. Rauschenbach, *Appl. Surf. Sci.* **253**, 6588 (2007)
19. K. Zimmer, R. Boehme, B. Rauschenbach, *J. Laser Micro Nanoeng.* **1**, 292 (2006)